Examining Ocean Mixing Dynamics at the Namonuito Guyot and Nam 2. Atoll

Ken Wilson

University of Washington, Seattle, WA

School of Oceanography

kjw13@uw.edu

3/14/2025

Abstract

This study investigates the impact of guyots and atolls on ocean currents and mixing processes in the Caroline Islands, Micronesia. The hypothesis is that atolls enhance vertical and horizontal mixing more effectively than guyots due to their surface-reaching morphology. To test this hypothesis, vertical profiling was conducted using underway CTD (Conductivity, Temperature, and Depth) and ADCP (Acoustic Doppler Current Profiler), along with calculations of mixed layer depth, stratification, mixing rate measurements, and Thorpe scale at Namonuito Guyot and an unnamed atoll near the guyot, referred to as Nam. 2 Atoll in this study. The findings reveal significant differences in mixing dynamics between the two features. The atoll exhibited stronger mixing and a more uniform mixed layer, driven by its interaction with surface currents and waves. In contrast, the guyot showed more stratified layers and weaker mixing, reflecting its submerged nature and limited interaction with surface processes. These results provide insights into the physical processes governing these geological features and their influence on ocean circulation, highlighting the distinct roles of guyots and atolls in shaping ocean mixing dynamics.

Plain Language Summary

This study compared two underwater features, guyots (submerged, flat-topped seamounts) and atolls (ring-shaped coral reefs surrounding lagoons), to understand their influence on ocean mixing. Using data from the Caroline Islands, the study found that atolls, with their surface-reaching structure, enhance water mixing more effectively than submerged guyots. This stronger mixing is driven by interactions with surface currents and waves, leading to a more uniform mixed layer. In contrast, guyots, being submerged, exhibit weaker mixing and more stratified layers due to their limited interaction with surface processes. These findings highlight the distinct roles of guyots and atolls in ocean dynamics and underscore the importance of their unique morphologies in shaping ocean circulation. The key takeaway: Atolls enhance ocean mixing through surface interactions, while guyots create more stable and stratified water columns.

Introduction

Guyots are significant underwater features that rise from the seafloor. These formations were once volcanic islands and are now isolated seamounts with flat tops, typically found at depths of 1,000 to 2,000 meters. Guyots and seamounts are very similar, with the key distinction that guyots were once islands that have since been submerged, whereas seamounts originate from the ocean floor and remain underwater. These geological structures play a crucial role in altering ocean currents and mixing processes. Other guyots have been studied in the western Pacific Ocean using CTD and ADCP data, where it has been found that as ocean currents encounter seamounts, they produce complex dynamic responses that can influence circulation patterns on both local and global scales (Wang et al., 2014). These dynamic processes near seamounts greatly contribute to local biological and sedimentary environments and facilitate mass and energy exchange in the deep ocean (Wang et al., 2014). This study focuses on the Namonuito Guyot and an unnamed atoll near the guyot, referred to as Nam. 2 Atoll in this study, in the Caroline Islands, Micronesia, examining mixing dynamics from the surface down to 500 meters to understand how these features influence ocean circulation and mixing.

On a broader scale, guyots contribute to the vertical and horizontal transfer of heat, carbon, and other biochemical substances, which are critical to global climate regulation. By facilitating the movement of heat and carbon between the surface and deep ocean, guyots play a key role in regulating Earth's climate system. Additionally, guyots act as obstacles to water currents, enhancing tidal dissipation. This friction influences global ocean circulation patterns, which in turn affect climate dynamics (Pitcher et al., 2007). As obstacles to flow, guyots also induce local currents that enhance upwelling, bringing nutrient-rich deep water to the surface and supporting marine ecosystems.

Atolls, on the other hand, are volcanic islands that surround a lagoon on the surface of the ocean. Atolls are very different from guyots, with their prominent features being a ring-shaped coral reef or a string of closely spaced small coral islands, enclosing or nearly enclosing a shallow lagoon. Atolls can change over time due to the accumulation of sand from surface waves and currents, while guyots transform primarily through underwater dynamics. Atoll islands are dynamic landforms that continually adjust their size, location, and elevation in response to changing boundary conditions (Steibl et al., 2023). However, there is limited information on atolls within the context of ocean currents and mixing processes. Because guyots and atolls have different morphological features, guyots being submerged while atolls rise to the surface, it is hypothesized that atolls enhance vertical and horizontal mixing of water more effectively than guyots. This is due to their direct interaction with surface waves, wind, and currents, which generate turbulence and disrupt stratification, leading to stronger mixing in the upper ocean. In contrast, guyots, being submerged, have limited interaction with surface processes, resulting in weaker mixing and more stable water columns. Understanding the interactions of ocean currents between guyots and atolls is fundamental to advancing knowledge of ocean dynamics and their role in global climate regulation.

The study was conducted in the Caroline Islands in Micronesia, as the tropical Western Pacific Ocean, a typically oligotrophic region with complex circulation, is an important area for studying these physical processes (Shi et al., 2021). Specifically, the research focused on Namonuito Guyot and Nam. 2 Atoll. There was very little information on Namonuito Guyot and no information on Nam. 2 Atoll, and this study aimed to fill that gap in the existing research.

There are several gaps in the existing understanding that this study aims to address. First, while the effects of guyots on ocean circulation and mixing processes are relatively well

documented, the understanding of how atolls, with their unique morphology and dynamics, influence these phenomena is limited. Applying this understanding to atolls will help predict similar patterns in different geological settings and improve models of oceanic processes. Additionally, there is no research on the atoll in this specific region, highlighting the importance of this study in providing regional insights. Second, the specific roles of guyots and atolls in these processes have not been comprehensively studied in terms of current dynamics. By analyzing how the differences in features between guyots and atolls affect currents and mixing, this research offers new insights into how two unique geological features alter the ocean. Lastly, the interactions between atoll dynamics and broader ocean circulation patterns have not been fully explored. This research investigates how atoll-induced mixing processes contribute to global ocean circulation, enhancing the understanding of their role in large-scale ocean dynamics. By addressing these gaps, this study contributes to a more comprehensive understanding of the complex interplay between geological features and oceanographic processes.

Methods

The study was conducted in the Caroline Islands in Micronesia. Fieldwork took place from December 31, 2024, to January 1, 2025. The research team traveled aboard the R/V Thomas G. Thompson, covering approximately 250 miles from Guam to Namonuito Guyot (9.9034° N, 148.3043° E to 9.6088° N, 148.3860° E) and Nam. 2 Atoll (9.0157° N, 147.9535° E to 8.8947° N, 147.7227° E) (Figure 1). The exact positions for the uCTD profiles and ADCP measurements were carefully documented.

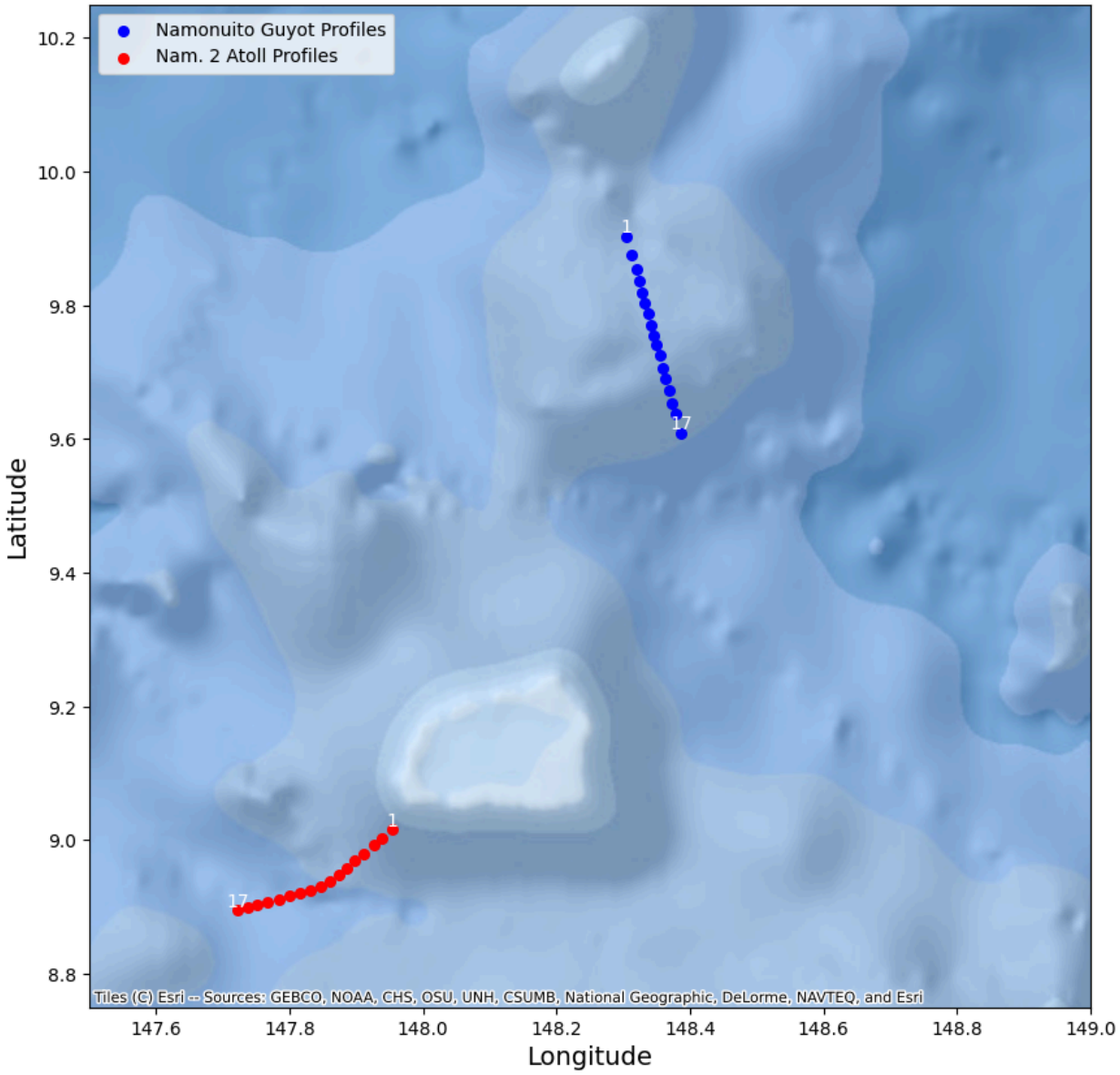

Figure 1. Map of uCTD Profile Locations. The map shows the profile locations for Namonuito Guyot (blue) and Nam. 2 Atoll (red). Coordinates for each profile are marked and labeled with their corresponding cast numbers from 1 and 17.

Vertical profiling was conducted using an underway Conductivity-Temperature-Depth (uCTD) instrument, which measures temperature, salinity, and density profiles. The uCTD was deployed from the ship while underway, allowing for rapid data collection with a fall rate of 100

meters per minute and a depth of approximately 500 meters for each profile. During deployment, the uCTD was lowered into the water using a winch system, and the instrument descended freely while transmitting real-time data to the shipboard computer. Deployment times, ship speed, and the uCTD fall rate were meticulously recorded to ensure precise data collection. Profiles were collected along the transect of Namonuito Guyot (Figure 2) and Nam. 2 Atoll (Figure 3). Additionally, Acoustic Doppler Current Profiler (ADCP) measurements were used to provide continuous data on current velocities at various depths. This allowed for the correlation of uCTD data with dynamic oceanic conditions, enhancing the understanding of mixing processes.

A total of 17 uCTD profiles were measured across Namonuito Guyot (Table 1), and 17 profiles were collected at least 1 nautical mile away from the shoreline of Nam. 2 Atoll (Table 2). All profiles extended to a depth of approximately 500 meters. Temperature and density profiles were used to determine the Mixed Layer Depth (MLD). The MLD was identified as the depth where temperature and density showed significant changes from the surface, using the algorithm described by de Boyer Montegut et al. (2003) and the Holte and Talley (2009) method.

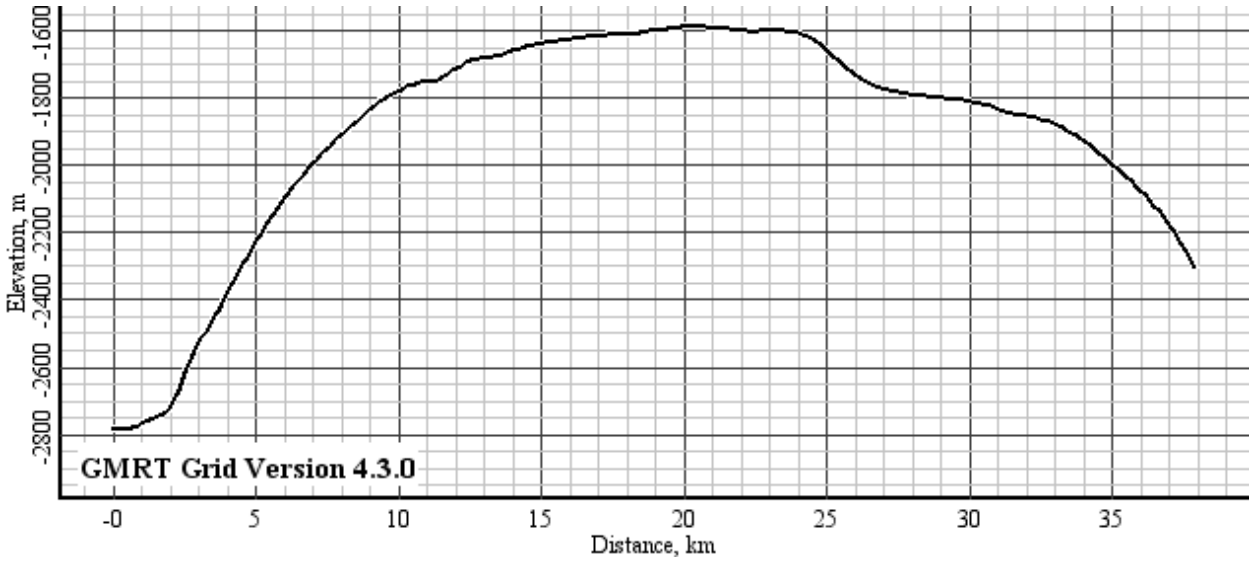

Figure 2. Elevation (m) and distance (km) of the Namonuito Guyot cross-section transect using GeoMapApp. The cross-section starts at 9.9034° N, 148.3043° E, and ends at 9.6088° N, 148.3860° E.

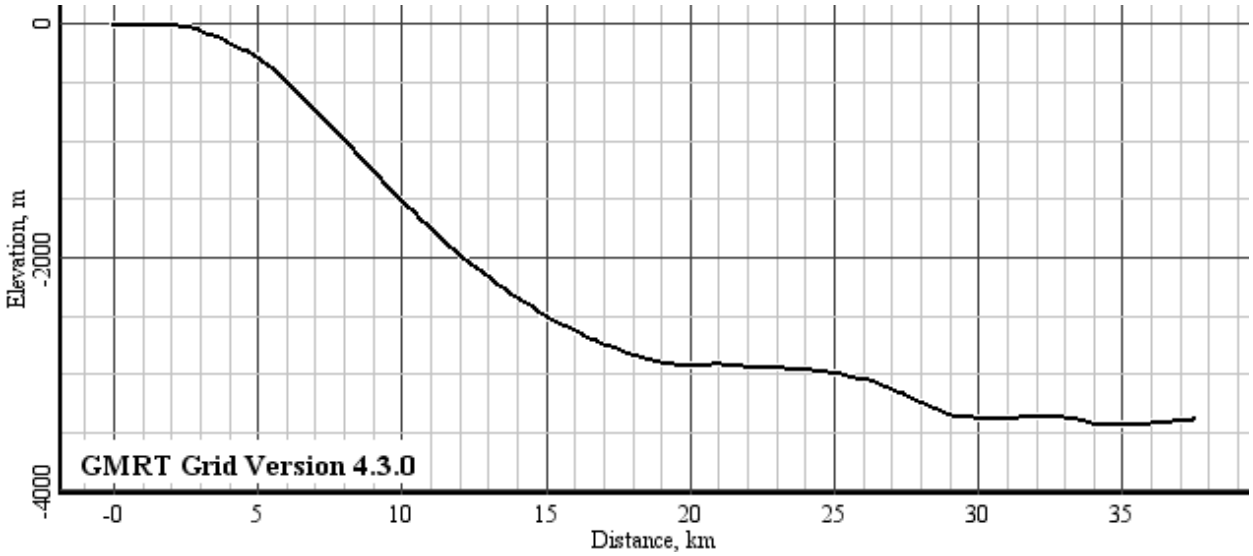

Figure 3. Elevation (m) and distance (km) of the Nam. 2 Atoll cross-section transect using GeoMapApp. The cross-section starts at 9.0157° N, 147.9535° E, and ends at 8.8947° N, 147.7227° E.

Table 1.

Namonuito Guyot uCTD Profiles (12/31/2024)

Order of uCTD Profiles	Location	Time (UTC)
Profile 1	9.9034° N, 148.3043° E	0:05
Profile 2	9.8750° N, 148.3126° E	0:33
Profile 3	9.8540° N, 148.3207° E	0:52
Profile 4	9.8357° N, 148.3234° E	1:08
Profile 5	9.8199° N, 148.3282° E	1:24
Profile 6	9.8041° N, 148.3324° E	1:39

Profile 7	9.7882° N, 148.3369° E	1:55
Profile 8	9.7703° N, 148.3415° E	1:55
Profile 9	9.7539° N, 148.3461° E	2:24
Profile 10	9.7401° N, 148.3496° E	2:37
Profile 11	9.7248° N, 148.3547° E	2:52
Profile 12	9.7058° N, 148.3592° E	3:10
Profile 13	9.6902° N, 148.3636° E	3:25
Profile 14	9.6726° N, 148.3692° E	3:40
Profile 15	9.6531° N, 148.3733° E	3:56
Profile 16	9.6381° N, 148.3781° E	4:10
Profile 17	9.6088° N, 148.3860° E	4:25

Table 2.

Nam. 2 Atoll uCTD Profiles (1/4/2025)

Order of uCTD Profiles	Location	Time (UTC)
Profile 1	9.0157° N, 147.9535° E	11:33
Profile 2	9.0022° N, 147.9389° E	11:46
Profile 3	8.9922° N, 147.9263° E	12:00
Profile 4	8.9800° N, 147.9115° E	12:18
Profile 5	8.9694° N, 147.8983° E	12:33
Profile 6	8.9588° N, 147.8853° E	12:47
Profile 7	8.9488° N, 147.8734° E	13:02
Profile 8	8.9380° N, 147.8604° E	13:17
Profile 9	8.9304° N, 147.8471° E	13:30
Profile 10	8.9252° N, 147.8320° E	13:44

Profile 11	8.9206° N, 147.8154° E	13:59
Profile 12	8.9162° N, 147.7997° E	14:13
Profile 13	8.9119° N, 147.7841° E	14:27
Profile 14	8.9072° N, 147.7671° E	14:42
Profile 15	8.9034° N, 147.7519° E	14:55
Profile 16	8.8991° N, 147.7380° E	15:09
Profile 17	8.8947° N, 147.7227° E	15:23

The MLD was calculated using temperature, salinity, and density profiles obtained from the uCTD data. The profiles were processed using the Python package GSW (TEOS-10). The MLD was determined by identifying the depth at which temperature, salinity, and density values showed significant changes from the surface, using an algorithm described by De Boyer Montégut et al. (2004) and applied to each uCTD profile. Thresholds of 0.2°C for temperature, 0.1 PSU for salinity, and 0.03 kg/m³ for density were used. A reference value was defined at a pressure of 10 dbar, and the MLD was identified as the depth where the observed value exceeded the reference value by the specified threshold. To facilitate visualization, the profiles were interpolated onto a regular grid using the SciPy library, creating contour plots that show temperature, salinity, and density variations with depth and time for both Namonuito Guyot and Nam 2. Atoll. The calculated MLDs were overlaid on the contour plots as dashed lines, providing a clear indication of the mixed layer depth for each figure.

Buoyancy frequency is crucial for understanding vertical water movement and overall ocean mixing. Stratification was evaluated by calculating the Brunt-Väisälä frequency (N), which indicates the stability of the water column. The frequency was calculated using the formula:

$$N = \sqrt{(-\ g/\rho 0\ *\ d\rho/dz)},$$

where g is the acceleration due to gravity, ρ0 is the reference density of seawater and $d\rho/dz$ is the density gradient with depth. The Python package GSW with TEOS-10 was used for inputting uCTD data and computing the Brunt-Väisälä frequency. The change in density with depth $\Delta\rho/\Delta z$ was directly calculated from uCTD profiles by computing the density gradient for depth, which involved evaluating the difference in density between two depths and dividing by the distance between them. Data points with sea pressure less than 3 dbar were filtered out to ensure accuracy. The calculated N^2 values were then plotted against pressure for both Namonuito Guyot and Nam 2. Atoll. Specific profiles were color-coded to highlight variations, helping to visualize the stability of the water column and identify regions of stratification.

Analyzing the ADCP data was conducted using Python in a Google Colab environment. The ADCP data, stored in NetCDF format, was accessed using the Xarray library. The process involved mounting the Google Drive to access the data file, followed by loading the ADCP data from the NetCDF file and extracting relevant variables such as time, depth, eastward velocity (u), and northward velocity (v). A depth mask was applied to limit the depth range to 0 to 800 meters, and the data was filtered accordingly. The depth data was oriented with 0 meters at the surface. Horizontal current speed was calculated using the Pythagorean theorem:

$$speed = \sqrt{(u^2 + v^2)},$$

and the direction of the current was determined using the arctangent function, with the result converted from radians to degrees. Contour plots were created using the Matplotlib library to visualize tidal flow variations. These plots depicted the current speed variations with depth and time at Namonuito Guyot and Nam 2. Atoll, using a consistent color scale ranging from 0 to 0.80

m/s to represent current speeds. The highest current speed calculated for ADCP was 0.80 m/s. The appearance of the plots was customized by setting axis labels, inverting the y-axis for depth, formatting x-axis labels for dates, and ensuring even increments for the color scale.

The Thorpe scale was calculated from uCTD data to obtain quantitative estimates of mixing rates. The Thorpe scale method, useful for analyzing vertical density profiles, involves rearranging an observed potential density profile into a stable monotonic profile without inversions. The displacement required to stabilize each sample is known as the Thorpe displacement (Dillon, 1982). The Thorpe displacement (d') was calculated as the difference between the initial and final depth of each sample. The Thorpe scale, Lt, was calculated using the formula:

$$Lt = \sqrt{\langle d'^2 \rangle},$$

where ⟨⟩ denotes the averaging process and d' is the Thorpe displacement of the initial depth (Zn) subtracted by the final depth (Zm) of each sample. Although the displacement (d') may not directly correspond to the actual travel distance of the sample, the Thorpe scale remains proportional to the average eddy size, provided that the mean horizontal density gradient is much smaller than the vertical gradient (Dillon, 1982). Profiles were interpolated onto a common pressure grid, and the mean Thorpe scale was calculated for each site. This method estimates mixing rates based on small density variations.

Results

The Namonuito Guyot transect displayed a current speed reaching approximately 0.4 m/s, concentrated around 100 meters in depth (Figure 4). Slower currents were observed at the edges

of the guyot, while faster flows were detected near the middle of the transect at this depth. At around 300 meters, current speeds of 0.3 m/s were observed starting from 02:24 UTC onward.

In contrast, the Nam. 2 Atoll transect exhibited the fastest current speeds near the surface, reaching approximately 0.8 m/s above 100 meters depth, with significant variations in speed observed throughout the water column. Notably, current speeds closer to the shore were consistently higher, averaging around 0.4 m/s, starting from 11:33 UTC onward. Additionally, moderate current speeds of approximately 0.3 m/s were observed at depths of around 300 meters, particularly from 12:47 UTC onward, further away from the shore.

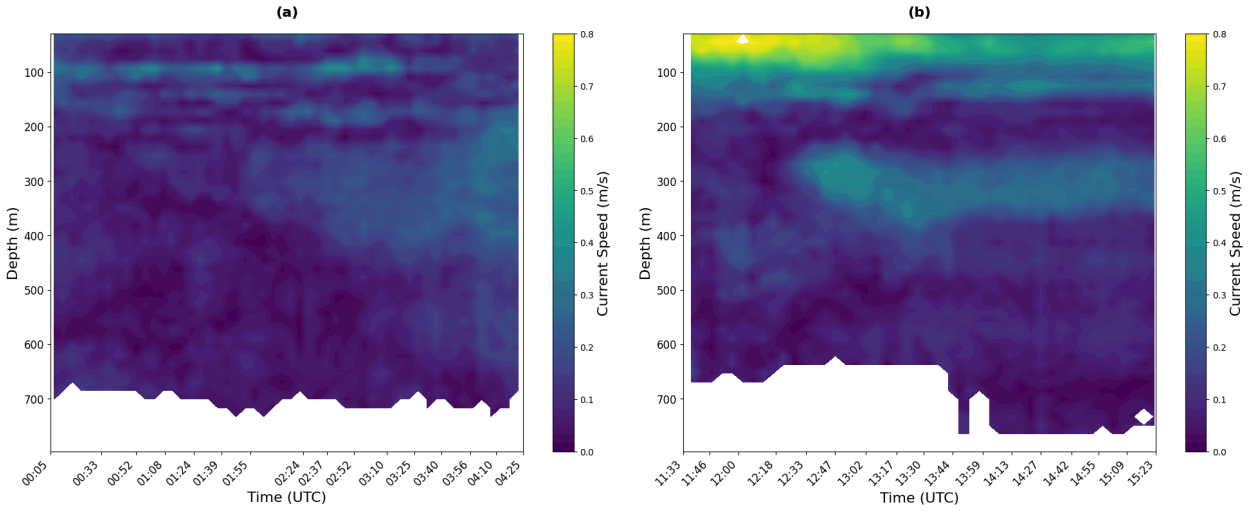

Figure 4. Tidal flow variations and current speed changes throughout the tidal cycle. Contour plots illustrating the current speed (m/s) variations with depth and time at (a) Namonuito Guyot and (b) Nam 2. Atoll, covering various phases of the mixed semidiurnal tidal cycle.

At Namonuito Guyot, the MLD for temperature was approximately 75 meters, while for salinity and density, it was shallower at around 25 meters (Figure 5). The highest temperatures

were observed near the surface, gradually decreasing with depth. Salinity exhibited its maximum values just below 100 meters, with the lowest salinity occurring at the surface between 0 and 75 meters, followed by a sharp increase between 75 and 150 meters. Density showed a consistent increase with depth, with a notable change starting from 100 meters downward. Additionally, the temperature displayed a deeper MLD at 00:05 and 00:33 UTC, all reaching the surface.

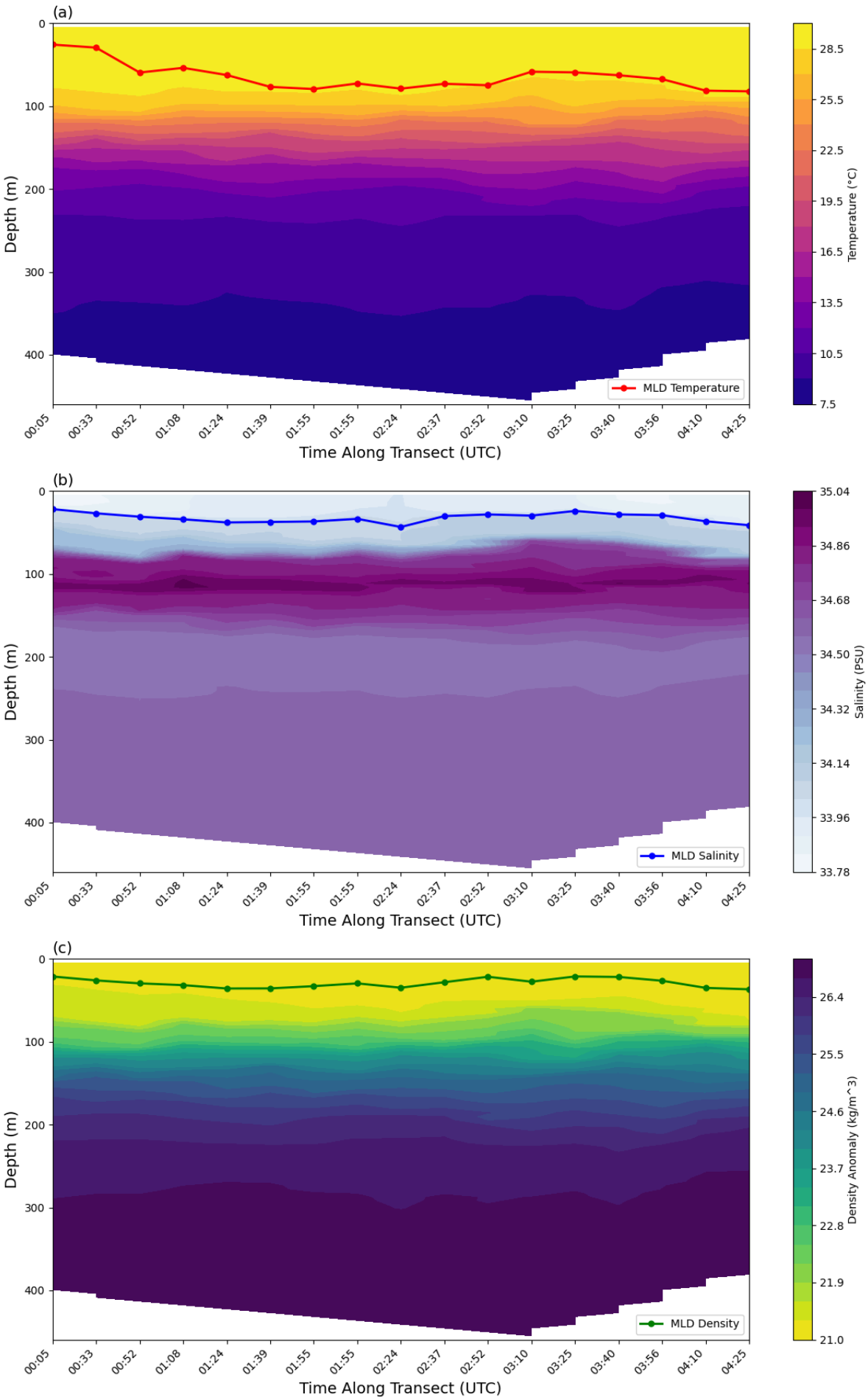
(a)
Depth (m)
0
100
200
300
400
MLD Temperature
00:05
00:33
00:52
01:08
01:24
01:39
01:55
01:55
02:24
02:37
02:52
03:10
03:25
03:40
03:56
04:10
04:25
Time Along Transect (UTC)
28.5
25.5
22.5
19.5
16.5
13.5
10.5
7.5
Temperature (°C)
(b)
Depth (m)
MLD Salinity
Time Along Transect (UTC)
35.04
34.86
34.68
34.50
34.32
34.14
33.96
33.78
Salinity (PSU)
(c)
Depth (m)
MLD Density
Time Along Transect (UTC)
26.4
25.5
24.6
23.7
22.8
21.9
21.0
Density Anomaly (kg/m^3)

Figure 5. Vertical profiles of (a) temperature, (b) salinity, and (c) density anomaly along the Namonuito Guyot transect, plotted as a function of depth (m) and time (UTC). MLD for each parameter is indicated by colored lines: red for temperature (threshold: 0.2°C), blue for salinity (threshold: 0.1 PSU), and green for density anomaly (threshold: 0.03 kg/m³).

For Nam. 2 Atoll, the MLD for temperature was approximately 70 meters, while for salinity, it was around 50 meters, and for density, it was 60 meters (Figure 6). Density and salinity exhibited higher values further from the shore, with salinity reaching as high as 35 PSU between 13:44 and 15:23 UTC, the farthest point from the atoll. The highest temperatures were observed at the surface, gradually decreasing with depth. Salinity peaked around 75 meters, with the lowest values occurring at the surface between 0 and 60 meters, followed by a sharp increase between 60 and 100 meters and a gradual decrease beyond this depth. Density was highest in the deeper layers, showing a sharp increase starting from 100 meters downward.

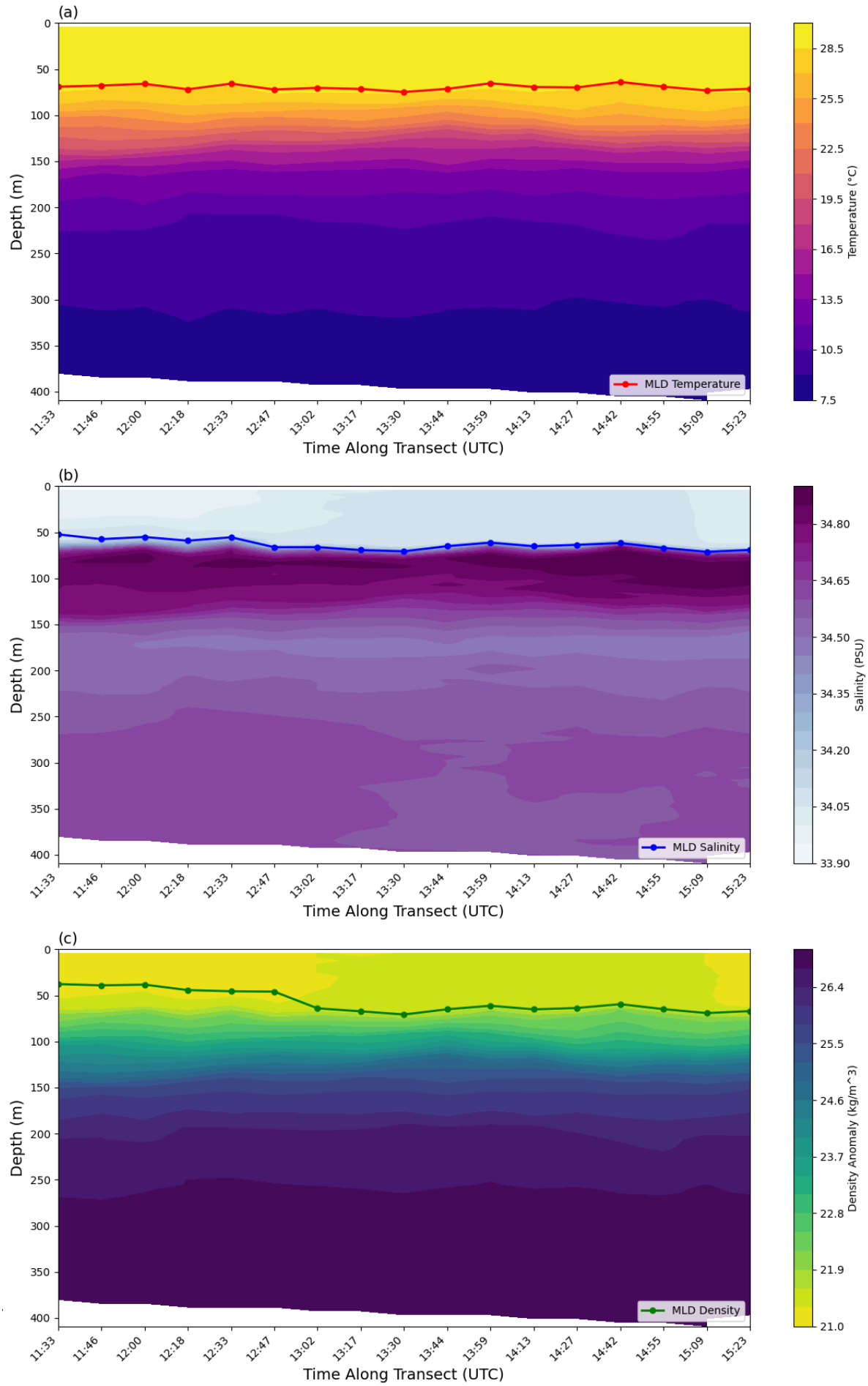
(a)
Depth (m)
Time Along Transect (UTC)
MLD Temperature
Temperature (°C)
(b)
Depth (m)
Time Along Transect (UTC)
MLD Salinity
Salinity (PSU)
(c)
Depth (m)
Time Along Transect (UTC)
MLD Density
Density Anomaly (kg/m^3)

Figure 6. Vertical profiles of (a) temperature, (b) salinity, and (c) density anomaly along the Nam. 2 Atoll transect, plotted as a function of depth (m) and time (UTC). MLD for each parameter is indicated by colored lines: red for temperature (threshold: 0.2°C), blue for salinity (threshold: 0.1 PSU), and green for density anomaly (threshold: 0.03 kg/m³).

For Namonuito Guyot, the mean buoyancy frequency squared (N^2) was highest between 80 and 200 dbar, reaching a maximum of approximately 0.0005 s^{-2} (Figure 7). The lowest frequencies were observed in the upper 0 to 50 dbar and below 200 dbar, with values less than 0.0001 s^{-2} in these depth ranges. In contrast, for Nam. 2 Atoll, the buoyancy frequency peaked between 50 and 150 dbar, with a maximum frequency of roughly 0.0007 s^{-2}. The lowest frequencies were similarly found in the upper 0 to 50 dbar and below 200 dbar, with values less than 0.0001 s^{-2}. The standard deviation (SD) of N^2 was larger for Namonuito Guyot between 50 and 200 dbar and for Nam. 2 Atoll between 75 and 150 dbar, indicating greater variability in stratification within these depth ranges.

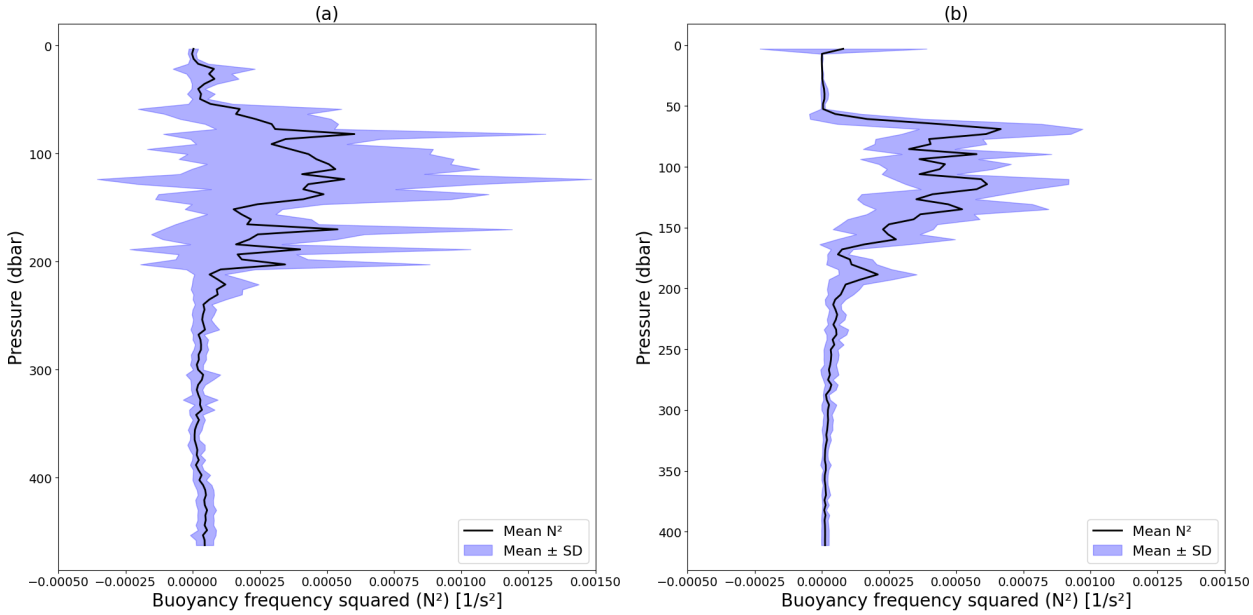

Figure 7. Brunt-Väisälä frequency squared (N^2) ($1/s^2$) profiles as a function of pressure (dbar) for (a) Namonuito Guyot and (b) Nam, 2 Atoll. Mean N^2 and its standard deviation (SD) are computed by interpolating all profiles onto a common pressure grid and averaging across the profiles.

For Namonuito Guyot, the Thorpe scale (Lt) showed the highest peak around 100 dbar (Figure 8). In contrast, for Nam. 2 Atoll, the Thorpe scale reached its highest peak of 0.6 meters, with the largest values observed between 8 and 120 dbar. Nam. 2 Atoll showed the least turbulence from 0 to 50 dbar, with Thorpe scale values as low as 0.001 meters in this depth range. Below 200 dbar, both features showed similar mixing dynamics, with Thorpe scale values gradually decreasing with depth.

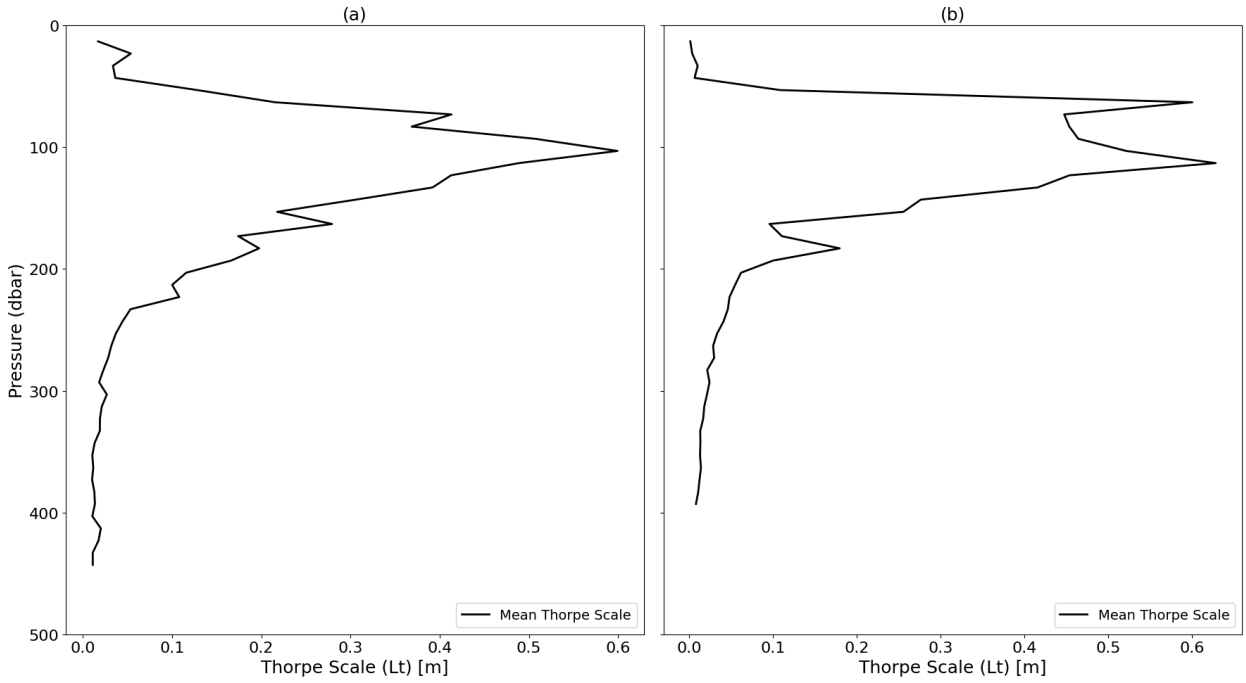

Figure 8. Thorpe scale (Lt) [m] profiles as a function of pressure (dbar) for (a) Namonuito Guyot and (b) Nam. 2 Atoll. Mean Lt and its variability are computed by interpolating all profiles onto a common pressure grid and averaging across the profiles.

Discussion

The observed differences in the MLD and buoyancy frequency between Namonuito Guyot and Nam 2. Atoll highlights the contrasting mixing regimes driven by their distinct morphologies. The guyot's more stratified salinity and density layers suggest weaker vertical mixing in the upper ocean, likely due to its submerged nature and limited interaction with surface currents. Because the guyot is entirely underwater, it does not interact directly with surface waves or wind, which are primary drivers of turbulence and mixing in the upper ocean. Instead, mixing around the guyot is primarily driven by internal waves and tidal currents, which are weaker compared to surface-driven processes.

In contrast, the atoll's uniform MLD indicates stronger mixing, attributed to its surface-reaching morphology and direct interaction with surface currents and waves. The atoll's ring-shaped structure disrupts surface flows, creating turbulence and enhancing vertical mixing. Wind and wave energy are transferred directly into the water column, breaking down stratification and creating a more uniform mixed layer. Additionally, the atoll's shallow lagoon and surrounding reef system further amplify mixing by channeling and accelerating tidal currents, which generate additional turbulence. This strong surface-driven mixing explains why the atoll exhibits a more uniform MLD and weaker stratification compared to the guyot.

These findings align with previous studies showing that ocean currents interacting with seamounts and guyots produce complex dynamic responses (Wang et al., 2014). The pronounced stratification and weaker mixing observed at Namonuito Guyot are consistent with these observations. Submerged features like guyots induce local currents and enhance upwelling, but their primary effect is to create a more stratified water column. This occurs because guyots, being submerged, do not interact directly with surface processes like wind and waves, which are

key drivers of turbulence and mixing. Instead, mixing around guyots is driven by weaker internal waves and tidal currents, leading to the stable and stratified water column observed in this study.

The Brunt-Väisälä frequency profiles further demonstrate the stability of the water column along both transects. While both features exhibit regions of strong stratification, the atoll's sharper transitions and higher frequencies in the upper ocean suggest more dynamic mixing processes near the surface. This is consistent with the atoll's exposure to surface waves and currents, which enhance turbulence and disrupt stratification. In contrast, the guyot's submerged nature leads to more pronounced stratification and weaker mixing in the upper ocean. These findings support the role of underwater features in enhancing tidal dissipation and influencing global circulation (Pitcher et al., 2007). The higher Brunt-Väisälä frequencies at the atoll align with the idea that surface-reaching structures enhance mixing, while the lower frequencies at the guyot reflect its limited interaction with surface processes. Additionally, the standard deviation of N^2 was much larger for the guyot, indicating greater variability in stratification, while the atoll's standard deviation was closer to the mean, reflecting more consistent mixing processes due to its surface interactions.

In addition to stratification, turbulence measurements using the Thorpe scale provided further insights into mixing dynamics. The Thorpe scale results, however, were somewhat unexpected. Despite the morphological differences between the guyot and atoll, the Thorpe scale values were surprisingly similar, with both features showing a peak in mixing around 100–200 meters. This suggests that internal waves and turbulence play a significant role in mixing at these depths, regardless of surface interactions. However, the atoll exhibited less turbulence near the surface (0–50 meters), which aligns with its highly stratified surface layer. This contrast

highlights the unique influence of surface processes at the atoll, even though deeper mixing dynamics were similar to the guyot.

These findings support the hypothesis that atolls enhance vertical and horizontal mixing more effectively than guyots, particularly near the surface. The stronger mixing at the atoll is driven by surface forcing mechanisms like wind and waves, which generate turbulence and disrupt stratification. The atoll exhibited a more uniform MLD of 70 meters for temperature, 50 meters for salinity, and 60 meters for density, compared to the guyot's MLD of 75 meters for temperature and 25 meters for salinity and density. Additionally, the atoll's stratification peaked at 0.0007 s^{-2} between 50 and 150 dbar, reflecting stronger mixing near the surface, while the guyot's stratification peaked at 0.0005 s^{-2} between 80 and 200 dbar, indicating more stable stratification. In contrast, the guyot's limited interaction with surface processes leads to weaker mixing and a more stable water column, as evidenced by its deeper MLD and lower stratification values in the upper ocean.

While these findings provide valuable insights, certain limitations must be acknowledged. The reliance on vertical profiling and indirect measurements of mixing, like the Thorpe scale, may not capture the full spatial and temporal variability of these processes. However, the use of uCTD and ADCP allowed for high-resolution measurements of temperature, salinity, density, and current velocities, providing detailed insights into mixing dynamics. Future studies could incorporate high-resolution numerical modeling or direct turbulence measurements, such as microstructure profiling, to further validate these findings. Additionally, expanding the study to include more guyots and atolls in different oceanic regions would help generalize these results and improve the understanding of how underwater features influence ocean dynamics on a global scale.

Conclusion

This study reveals significant differences in the ocean mixing dynamics at Namonuito Guyot and Nam 2. Atoll, driven by their distinct morphologies and interactions with ocean currents. While it may seem intuitive that atolls enhance mixing more effectively than guyots due to their surface-reaching structure, this research provides quantitative evidence of how and why this happens. The atoll exhibited stronger mixing and a more uniform mixed layer, consistent with its exposure to surface waves and currents, while the guyot showed more stratified layers and weaker mixing, reflecting its submerged nature. These findings not only confirm the expected differences but also provide new insights into the mechanisms driving these processes. By quantifying how guyots and atolls influence ocean mixing, this study contributes to a better understanding of ocean circulation, heat transport, and climate regulation, offering a foundation for future research and improving climate models.

References

De Boyer Montégut, Clément, et al. (2004). Mixed layer depth over the global ocean: An examination of profile data and a profile‐based climatology. Journal of Geophysical Research: Oceans, vol. 109, no. C12. https://doi.org/10.1029/2004jc002378.

Dillon, T. M. (1982). Vertical overturns: A comparison of Thorpe and Ozmidov Length Scales. Journal of Geophysical Research: Oceans, 87(C12), 9601–9613. https://doi.org/10.1029/jc087ic12p09601

Goldberg, J., & Rankley, E. C. (2023). The Atolls of the Caroline Islands. In A Global Atlas of Atolls (pp. 181–204). https://doi.org/10.1201/9781003287339

Hautala, S. (2020). Stratification and buoyancy forces. Physics across oceanography fluid mechanics and waves. uw.pressbooks.pub/ocean285/chapter/stratification-and-buoyancy-forces/

Holte, J., & Talley, L. (2009). A new algorithm for finding mixed layer depths with applications to Argo data and Subantarctic Mode Water formation. Journal of Atmospheric and Oceanic Technology, 26(9), 1920–1939. https://doi.org/10.1175/2009JTECHO543.1

Mashayek, A., Gula, J., Baker, L. E., & Lavergne, C. (2024). On the role of seamounts in upwelling deep-ocean waters through turbulent mixing. Proceedings of the National Academy of Sciences, 121(27). https://doi.org/10.1073/pnas.2322163121

Pickering, A. (2016). Ocean Mixing Community. Standard Mixing Routines [Software]. GitHub. https://github.com/OceanMixingCommunity/Standard-Mixing-Routines/tree/master/ThorpeScales

Pitcher, T. J., Morato, T., Hart, P. J. B., Clark, M. R., Haggan, N., & Santos, R. S. (Eds.). (2007). Seamounts: Ecology, fisheries & conservation. https://doi.org/10.1002/9780470691953

Shi, X., Wang, Z., & Huang, H. (2021). Physical oceanography of the Caroline M4 seamount in the tropical Western Pacific Ocean in summer 2017. Journal of Oceanology and Limnology, 39(5), 1634–1650. https://doi.org/10.1007/s00343-021-0359-8

Steibl, S., Kench, P. S., Young, H. S., Wegmann, A. S., Holmes, N. D., Bunbury, N., Teavai-Murphy, T. H., Davies, N., Murphy, F., & Russell, J. C. (2023). Rethinking atoll futures: Local resilience to global challenges. Trends in Ecology and Evolution, 39. https://doi.org/10.1016/j.tree.2023.11.004

Wang, Z., Shi, X., & Huang, H. (2022). Observation of physical oceanography at the Y3 seamount (Yap arc) in winter 2014. Journal of Oceanology and Limnology, 40(4), 1314–1332. https://doi.org/10.1007/s00343-021-1164-0

Use of AI

This thesis utilized ChatGPT to assist with grammar, flow, and clarity improvements. All ideas, analysis, and interpretations are original work. Additionally, ChatGPT was used to troubleshoot code for data analysis.